DALTON

Covalence and spin polarisation in tetraphenylarsonium tetrachloronitridotechnetate(VI) studied by polarised neutron diffraction†

Philip A. Reynolds,*[a] Brian N. Figgis,[b] J. Bruce Forsyth[c] and Francis Tasset[d]

[a] *Research School of Chemistry, Australian National University, Canberra, ACT 0200, Australia*
[b] *Department of Chemistry, University of Western Australia, Nedlands, WA 6907, Australia*
[c] *ISIS facility, Rutherford-Appleton Laboratory, Chilton, Didcot, Oxon. OX11 0QX, UK*
[d] *Institut Laue-Langevin, Avenue des Martyrs, Grenoble 38042, France*

Polarised neutron diffraction from two orientations of tetragonal single crystals of $[AsPh_4][TcNCl_4]$ at 1.5 K and a magnetic field of 4.6 T gave a combined data set of 116 magnetic structure factors. These were fitted by a 26-parameter model which includes proton nuclear-spin orientation to give a spin-density model for the formally $4d^1$ $[TcNCl_4]^-$ ion. This model revealed substantial anisotropic π bonding between Tc and Cl resulting in 29(2)% of the spin being delocalised onto the chlorine in-plane $3p_\pi$ orbitals, −15(1)% onto the nitrogen as a result of spin-polarising the short Tc–N bond, and substantial spin polarisation on the technetium site of 4d and more diffuse density. Three unconstrained Hartree–Fock and density functional calculations with good basis sets failed to reproduce these observations adequately, but an unconstrained density functional calculation with gradient corrections and a relativistic treatment of the core gave encouraging agreement with experiment.

Studies of bonding in metal complexes have predominantly been based on spectroscopic techniques. Since magnetic properties arise mainly from the valence electrons they are very sensitive to changes in bonding. Spectroscopic techniques examining magnetic behaviour, such as ESR, are particularly informative. On the other hand, diffraction study of the magnetic properties by polarised neutron diffraction (PND) probes the spatial rather than energetic aspects of the wavefunction and highlights different features of the bonding. This has proved useful for complexes of the first transition series in defining the balance of factors such as covalence, electron correlation, and the influence of spin–orbit coupling, in both ionic and covalent systems.[1]

We have begun PND studies of complexes involving transition metals of the second and third series, thus far including $[Ru(acac)_3]$[2], (acac = acetylacetonate) tetrachlorobis(*N*-phenylacetamidino)rhenium,[3] and a molybdenum(III) alum.[4] The first two have interesting properties which are much modified by intermolecular exchange, while the latter is quite ionic in nature. In the present context, we searched for a highly covalent complex composed of magnetically isolated units, so that we might test molecular theories of bonding in heavier metal systems. In particular, these heavier systems are expected to be more covalent than those of the first transition series, but simultaneously it is well recognised that the results of *ab-initio* calculations are less reliable. The salt $[AsPh_4][TcNCl_4]$ is, as we shall see, a more suitable complex for this particular purpose than others have been. First, previous work is reviewed to show why we suppose that this is so. We then introduce the effects of proton nuclear-spin polarisation, a complication which occurs in this material, but the effects of which can be well accounted for in the experiment. Our new PND results are then presented, some new theoretical *ab-initio* calculations are reported, and we compare them.

† *Supplementary data available* (No. SUP 57216, 4 pp.): magnetic structure factors. See Instructions for Authors, *J. Chem. Soc., Dalton Trans.*, 1997, Issue 1.
Non-SI units employed: $\mu_B \approx 9.27 \times 10^{-24}$ J T^{-1}, au $\approx 4.36 \times 10^{-18}$ J.

Previous work on $[TcNCl_4]^-$ salts

(*a*) Crystal structure of $[AsPh_4][TcNCl_4]$

This crystal has been examined by single-crystal X-ray diffraction to obtain structures at 293,[5] at 120 K,[6] and by neutron diffraction at 28 K.[6] There are no phase changes, and the crystal remains tetragonal at all temperatures with a cell $a = 12.55(1)$, $c = 7.70(1)$ Å at 28 K. The cation and anion both exhibit a four-fold symmetry axis, C_4 and S_4 respectively. The tetraphenylarsonium ion is, as expected, of propeller-like conformation, while the $[TcNCl_4]^-$ ion is a square pyramid with a Tc–N distance of 1.625(4) Å and a Tc–Cl distance of 2.335(3) Å with an N–Tc–Cl angle of 103.3(1)°. The cation and anion are linked by H · · · Cl contacts. The unit-cell contents are illustrated in Fig. 1, which is a projection down the four-fold axis of this tetragonal crystal. We note that the Tc–N bond is parallel to this axis.

(*b*) Bulk magnetic properties of $[AsPh_4][TcNCl_4]$

Single-crystal susceptibility and magnetisation measurements have been reported down to a temperature of 4.5 K and up to a magnetic field of 5 T.[6] The behaviour is very simple: isotropic with a *g* factor of 2.00, and a small antiferromagnetic exchange term as defined by the Curie–Weiss plot with θ −0.13(5) K.

(*c*) Electron spin resonance on $[AsPh_4][TcNCl_4]$

Extensive ESR, electron–nuclear double resonance, and electron spin-echo envelope modulation experiments have been performed and interpreted.[5,7–9] Both hyperfine and nuclear quadrupole couplings have been extracted from the data.

(*d*) PND on $[AsPh_4][TcNCl_4]$

Six magnetic structure factors were obtained previously from a small crystal mounted with the *c* axis perpendicular to the basal plane of the diffractometer.[10] In this orientation the spin on Tc and N is not distinguishable, and so a simple one-parameter model with spin on Tc + N, and on Cl ligands, was fitted to these data.

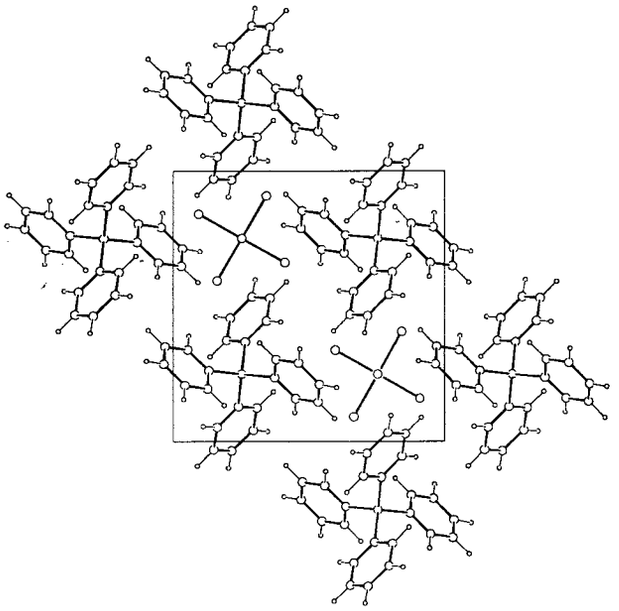

Fig. 1 Unit cell of $[AsPh_4][TcNCl_4]$ in *ab* projection

(*e*) Electronic theory

The electronic structures of square-pyramidal MXY_4^{n-} ions have been extensively studied theoretically by *ab-initio* methods, and the fundamental qualitative features of the bonding are now thought to be understood. Many of the calculations do not incorporate electron–electron correlation, such as may be introduced by, for example, using configuration interaction or unrestricted methods. We do not pursue these uncorrelated restricted calculations further, since, as will be seen, they cannot even reproduce the qualitative features that are observed in this experiment. There are two unrestricted calculations on the $[TcNCl_4]^-$ ion, one a neglect of diatomic differential overlap Hartree–Fock treatment[8] and one using a local density functional method.[10] More fundamentally, existing *ab-initio* calculational packages cannot extract spin densities from multideterminant wavefunctions, so only the unrestricted methods are immediately available for comparison.

(*f*) Current understanding of the bonding

The small magnetic exchange in the crystal suggests that a good model is to consider the crystal wavefunction as constructed essentially from isolated $[TcNCl_4]^-$ and $[AsPh_4]^+$ units. However, because of electrostatic and other effects these, at least in principle, differ from free-ion wavefunctions. The *ab-initio* calculations indicate that the naive view of a very strong Tc–N and a weaker Tc–Cl bond is reasonable. Given the large spin–orbit coupling constant for Tc^{6+}, *ca.* 1700 cm^{-1}, we would not expect a simple isotropic *g* tensor of value 2.00 to arise from such a ligand field. Indeed in related molecules there is both anisotropy and departure from 2.00 for the diagonal elements of the *g* tensor. In this case the isotropy, at least down to 4.5 K, seems to be a fortuitous result of the various covalences and spin–orbit coupling of Tc and Cl.[5] However we should be aware that at lower temperatures and high magnetic fields departures from a simple spin $\frac{1}{2}$ Brillouin function may occur in the bulk magnetisation.

Electron spin resonance spectroscopy and theory both agree in locating the bulk of the magnetisation in the technetium $4d_{xy}$ orbital in the *ab* plane. Both theory and ESR hyperfine coupling values indicate that this is also covalently delocalised onto the ligand *ab* plane chlorine 3p orbital. The axes are defined below in the section describing the modelling. A simple interpretation of the ESR results suggests 20% of the spin is on the chloride ligands. The ESR nuclear quadrupole coupling, and theory, suggest a substantial spin polarisation of the Tc–N bond, such that negative spin resides on the N atom and matching extra positive spin around the technetium atom.

While convincing quantitative data may be lacking, the agreement of simple molecular orbital ideas of bonding, more sophisticated *ab-initio* methods, and the ESR results might lead us to believe that that is essentially a complete description. Thus it was a surprise when the previous PND experiment apparently gave 45(6)% of the spin on the chlorines, more than twice the ESR value. Evidently the situation is more complex than was believed! The new PND results below confirm this.

PND on Systems Containing Polarised Proton Nuclear Spins

When proton nuclear spins are aligned along the applied magnetic field the effect on the PND experiment is straightforward. Extra interference terms between nuclear spin polarisation and both the nuclear and magnetic structure factors appear in the scattered intensity.[11] The nuclear spin–magnetic interference term is small and we shall neglect it. The nuclear spin–nuclear structure factor term appears in the effective magnetic structure factor as an apparent magnetic contribution of $5.402Pp/\cos^2\Omega\,\mu_B$, from each proton site, with a thermally smeared delta function form factor; *P* is the nuclear polarisation at the proton site, *p* the neutron polarisation, and Ω the angle between the normal to the neutron scattering plane and the vertical direction (in the usual experimental configuration). This nuclear spin effect on the PND experiment is due to the neutron–proton nuclear interaction being very different in the singlet and triplet states. A much more common manifestation of this is the very large proton incoherent scattering cross-section compared to other elements. Thus, even if other nuclei are polarised in this crystal to comparable amounts, the scattering change which results is much smaller. The incoherent scattering cross-section for technetium is not known, but is small compared to that for the proton. Nuclear scattering differs from magnetic scattering in that, because it is a contact term, there is no dependence on the angle between the neutron momentum transfer and the direction of polarisation. In the magnetic case there is a strong dependence of the observed flipping ratio on the lifting angle of the diffractometer. This makes magnetic and polarised nuclear scattering experimentally separable. However we do not present this separation, as when it was attempted the data were insufficiently extensive to give reliable results. There is also an extra truly magnetic nuclear polarisation term of $1.52 \times 10^{-3}Pp\,\mu_B$ due to the magnetic scattering from the nuclear magnetic moment, but here this is negligible.

This nuclear polarisation effect has not often been observed, but there are two classic experiments which show that the theory is indeed straightforward to apply. Abragam *et al.*[12] observed it in LiH by brute-force methods, producing proton nuclear spin polarisation of 0.183% (and lithium-6 polarisation of 0.036%, and ^{7}Li of 0.118%) by applying a magnetic field of 2.07 T at a temperature of 1.15 K. We note a typographical error in this paper of a factor of 10 in the quoted polarisations, though this is not carried further through the paper. We have checked all polarisations by appropriate calculations from nuclear moments, and $S = \frac{1}{2}$, 1 and $\frac{3}{2}$ Brillouin functions. Secondly Leslie *et al.*[13] performed PND experiments on a neodymium-doped lanthanum magnesium nitrate hydrate crystal in which the water protons were oriented by microwave pumping and use of the Overhauser effect. They succeeded in locating protons in the unit cell using the observed flipping ratios. More recently, various PND data on hydrogen-containing materials have required correction, and the subsequent successful refinement of these data indicates the accuracy of this correction process, *e.g.* ref. 14.

Experimental

A deep orange-red single crystal (60 mg) of $[AsPh_4][TcNCl_4]$, of prismatic habit, of length 10 mm along *c*, and *ca.* 1.5 × 1.5 mm in cross-section, from an earlier preparation and growth,[5] was mounted on the D3 lifting-arm polarised neutron diffractometer at the Institut Laue-Langevin in Grenoble. Two sets of measurements were made, one with [1 − 10] and one with [001] parallel to within 2° to the vertical applied magnetic field. The restrictions imposed by the lifting-arm geometry mean that with a single-crystal orientation we can reach reflections up to about 25° out of the diffractometer basal plane. The cell dimensions found [$a = 12.55(6)$, $c = 7.69(5)$ Å] are in excellent agreement with the 28 K result [$a = 12.55(1)$, $c = 7.70(1)$ Å], although less precise due to the relaxed resolution required for efficient PND data collection. The neutron wavelength obtained from the Heussler alloy monochromator was 84.3(1) pm, the polarisation ratios were $p_+ = 0.965(1)$ and $p_- = 0.974(1)$, and the flipping efficiency was 1.000(1). An erbium filter was used to reduce λ/2 contamination to 0.14(2)%.

The flipping ratios, *R*, of 290 and 270 reflections in the two orientations were measured at an applied magnetic field of 4.61 T at a sample temperature of 1.5 K. Each unique reflection was generally measured at three equivalent positions. The reflections measured were chosen as those with large nuclear structure Bragg intensities, giving relatively unbiased sampling of the magnetic structure factors in the experimentally accessible region of reciprocal space. We assume the magnetic and nuclear structure factors are not closely correlated. The flipping ratios were converted into magnetic structure factors using the neutron diffraction structure from Figgis *et al.*,[6] assuming the collinear magnetisation expected for this magnetically isotropic system. If polarised nuclear scattering is present the derived 'magnetic structure factors' are effective numbers, rather than the *z* components of the magnetic structure factor. The relevant expression is (1) where *R* is the observed flipping ratio for the

$$F_{\mathbf{M}} = F_{\mathbf{N}}([p(R + 1)/(R - 1)] \pm \{[p(R + 1)^2/(R - 1)^2] - (1/\sin^2 \Omega)\}^{\frac{1}{2}}) \quad (1)$$

reflection and $F_{\mathbf{N}}$ and $F_{\mathbf{M}}$ are the nuclear and magnetic structure factors respectively.

The data were symmetry averaged to 92 and 68 unique reflections in each orientation. These had 44 reflections in common, which were averaged to a final set of 116 reflections. When polarised protons are present, equivalent reflections at different experimental lifting angles are no longer exactly equivalent, both within and between the two data sets. However test calculations showed that this effect is distinctly smaller than the reduction in error to be made by such averaging. The data error estimates were derived from counting statistics, differences between equivalents, and an estimate of the error in $F_{\mathbf{N}}$. The final data range in (sin θ)/λ from 0.07 to 0.78 $Å^{-1}$, with $\Sigma\sigma(F_{\mathbf{M}})/\Sigma F_{\mathbf{M}} = 0.17$, and $\sigma(F_{\mathbf{M}})/F_{\mathbf{M}}$ as low as 0.03.

Results and Refinements

We fitted the observed effective magnetic structure factors by a model including both the polarised nuclear and magnetic scattering using a modified version of the program ASRED.[15] Polarised nuclear scattering was considered only from the protons. The magnetic scattering has been fitted by multipole models for the magnetisation density.

The initial model was given substantial flexibility so that the total magnetisation density could be fitted as well as possible, at the expense of possible large correlations between the fitting parameters. The second model, based on parameters seeming important from subsequent theoretical considerations, with fewer parameters, allows, at the expense of a marginally poorer fit, discussion in chemical terms of the major features contributing to the magnetisation density.

Table 1 Values of the fitted population parameters for the multipole model (units e). Multipoles are labelled (*nm*)

Atom	4d		4d′ *	
Tc	$4d_{xy}$	1.04(15)		−0.19(15)
	$4d_{xz + yz}$	−0.38(18)		0.40(18)
	$4d_{x^2 + y^2}$	0.26(15)		−0.18(15)
	$4d_{z^2}$	0.28(20)		−0.24(19)
	(10)	−0.08(2)		
	(30)	−0.02(5)		
		5s		
	(00)	−0.21(7)	(10)	0.00(4)
	(20)	0.23(7)	(30)	0.09(5)
	(40)	−0.26(8)	(44)	0.05(11)
Cl	(3sp)1	−0.017(7)	(3sp)2	−0.004(4)
	$3p_z$	0.021(4)	$3p_y$	0.070(5)
N	(2sp)1	−0.06(2)	(2sp)2	−0.01(1)
	$2p_\pi$	−0.06(2)	(30)	−0.01(3)
H	1s	0.002(2)		

* A function with contracted radius; $r_{4d'} = 0.7\ r_{4d}$.

For the radial dependence of the atomic contributions to the magnetisation density we have used Hartree–Fock solutions[16] for the 4d and 5s orbitals of the ^7S state of $4d^5 5s^1$ Tc^+, 3p for ^2P Cl^0, 2p for ^4S N^0, and the hydrogen 1s valence function of Stewart *et al.*[17] In addition, to provide sufficient flexibility in the fitting, it was necessary to add a contracted 4d function on the technetium site, 4d′, with radial functions $r_{4d'}$ of 0.7 r_{4d}. No angular dependence was used on the hydrogen sites, four multipoles on the Cl (all to order 2 assuming *mm* symmetry), four on N (all to order 3 using S_4 crystal site symmetry), and six each on the 4d and 5s technetium function radial dependences (all to order 4 in the C_4 crystal site symmetry), and five angular functions for the contracted 4d function on Tc (all the d-like dependences). All the five independent hydrogen sites were constrained to have equal 1s populations and nuclear polarisations. Many of the multipoles have been recast into linear combinations with simple chemical significance without loss of generality. Examples are those representing the d_{xy} and sp hybrid orbitals. This enables us to judge the importance of those populations which simple chemical models predict as being important. Some of the multipoles are not present in these simple chemical schemes and have been retained as unaltered multipoles. The axis systems are: Tc, $+z$ points along the four-fold axis towards N, $+x$ perpendicular to the four-fold axis along the projection of the Tc–Cl bond on the *ab* plane (thus $4d_{xy}$ is in the *ab* plane with lobes pointing between the Tc–Cl bonds); N, $+z$ towards Tc along the four-fold axis [thus (2sp)1 is an sp hybrid with its major positive lobe pointing towards Tc while (2sp)2 points away from Tc]; Cl, $+x$ along the Cl–Tc bond and $+y$ in the *ab* plane perpendicular to this [thus (3sp)1 points its major lobe towards Tc and $3p_y$ is a π bonding 3p in the *ab* plane].

This gives a total of 26 parameters used in the least-squares fit, and thus an observable:parameter ratio of 4.5:1. In addition the total magnetisation per unit cell was constrained to 2.00 $\mu_{\mathbf{B}}$, *viz.* magnetic saturation for $g = 2.00$.[6] The resulting fit gave the spin-population parameters of Table 1 with agreement factors of $R(F) = 0.083$, $R_w(F) = 0.024$ and goodness of fit, χ^2, of 0.69. The fitted value of the proton nuclear polarisation is 0.278(14)%. A list of observed and calculated magnetic structure factors has been deposited as SUP 57216. In Figs. 2 and 3 we show contour maps of the total magnetisation density in a Cl–Tc–Cl plane and a Cl–Tc–N plane. These were constructed by Fourier summation to a (sin θ)/λ limit of 1.2 $Å^{-1}$.

We tried variation of the model in a number of ways, but none gave significant improvement. They included (1) making all the hydrogen sites independent, (2) increasing the number of multipoles on N and Cl to four and/or allowing radial flexibility by use of a κ parameter, (3) introducing mid-bond Tc–N and

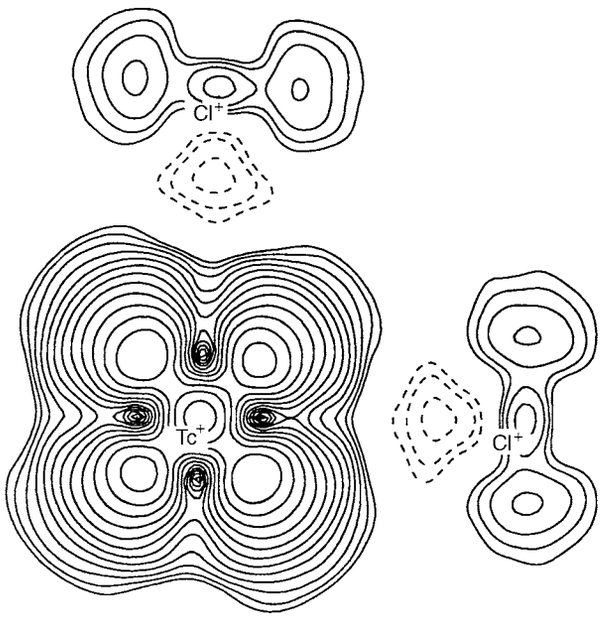

Fig. 2 Modelled spin density in a $TcCl_2$ plane of the $TcNCl_4$ fragment. The positive contours start at 0.01 μ_B Å^{-3}, increasing geometrically by $2^{\frac{1}{2}}$ for each contour, negative at −0.01 decreasing similarly

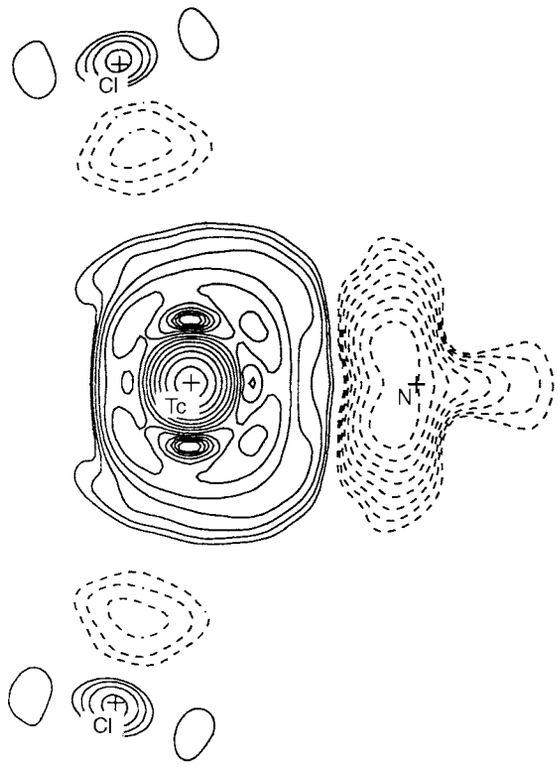

Fig. 3 Modelled spin density in a $TcNCl_2$ plane of the $TcNCl_4$ fragment. Contours as Fig. 2

Tc–Cl density functions, (4) introducing an extra hydrogen contracted radial function, (5) introducing populations on carbon and arsenic sites, and (6) independent refinement of the two data sets, *i.e.* assuming the magnetisation density differs between the two crystal orientations.

In our simplified 'chemical' model we have been guided by the theoretical results given below. These show no significant 5s or 5p spin components, a polarised very diffuse 4d density, 4d*, while the more contracted 4d density remains unpolarised and atom-like in radial distribution. Thus we removed both the contracted 4d density and the 5sp hybrids on Tc from our model and replaced them by a very diffuse 4d* density function, while retaining the atom-like technetium 4d function. The diffuse 4d* density, starting from the same radial distribution as the theoretical 5s, was allowed to change in radius with a κ parameter. We retained both hydrogen parameters, the polarised proton scattering and the 1s term. Also retained was a total of five independent p orbitals on N and Cl, and the (10) multipole on Tc. This gave a total of 18 parameters and a resulting fit of $R(F) = 0.092$ and $\chi^2 = 0.76$. The resulting parameters are summarised in Table 2 and given in detail in Table 3. It is clear that this chemical model encompasses the most important features although the more complete model is marginally better in fit.

Theoretical Calculations

In the theoretical treatment, a convenient benchmark is the scheme of Neuhaus *et al.*[18] who calculated the properties of many oxo- and nitrido-halogeno complexes of Mo, W, Re and Os. We have used exactly their *ab-initio* scheme to calculate the wavefunction of the $[TcNCl_4]^-$ ion. This involves a restricted open-shell Hartree–Fock (ROHF) calculation using the quasi-relativistic effective core potential of Hay and Wadt[19] with split-valence technetium basis set 441/2111/31 of Jonas *et al.*[20] and 3-21G(d) for Cl and 6-31G(d) for N.[21] Using GAMESS[22] we optimised the geometry in C_{4v} symmetry, giving a Tc–N bond length of 1.557 78 Å [experimental = 1.625(4) Å], Tc–Cl of 2.398 84 Å [experimental = 2.335(3) Å], an N–Tc–Cl bond angle of 102.165° [experimental = 103.3(1)°] and an energy of −1963.558 78 au. This reproduces the experience of Neuhaus *et al.* in that the metal–halide bond is calculated too short and the M–N or M–O bond too long. This ROHF calculation cannot, since spin resides in a single molecular orbital, give negative spin density on the nitrogen atom or anywhere else. However, the latter is one of the main observations of our experiment. Accordingly, as a minimum-level calculation with any hope of agreement with experiment, we performed an unconstrained Hartree–Fock (UHF) calculation, using the experimental molecular geometry. This gave an energy of −1963.550 88 au and some of the spin populations are listed in Table 2. Optimising the geometry gave results very close to those from the ROHF calculation.

We also performed a further Hartree–Fock calculation as different as we could from the previous one. This was an all-electron UHF calculation using the MIDI Gaussian basis set with two d-function polarisation functions on Cl and N [exponents 1.028 and 0.257 (Cl) and 1.728 and 0.432 (N) au],[23] and gave a total energy of −6073.9642 au at the experimental geometry.

We have also quoted in Table 2 the results of the local density functional (LDF) calculation of Figgis *et al.*,[10] which was a non-relativistic, all-electron, calculation with no gradient corrections. The basis set is derived from the numeric solutions of the free ions, and is thus inflexible in the molecular calculation. As an improvement on this we performed an unconstrained calculation at the experimental geometry using the Amsterdam density functional package[24] with the VWN local density approximation, Becke–Perdew gradient corrections, and frozen relativistic atomic cores. The Slater basis is roughly of triple-zeta flexibility. We also optimised the geometry and obtained a Tc–N distance of 1.6485 Å, Tc–Cl of 2.370 Å, and an N–Tc–Cl angle of 103.4°. These values are more than twice as close to experiment as those calculated by the ROHF method, and, given the possible compressible effects of crystal-packing forces, are perhaps as close as may be expected. Spin populations are listed in Tables 2 and 3. The three 4d-basis function populations have been collapsed to an atom-like 4d and a diffuse 4d*. We calculated an 'expected' diffuse atom-like component from the molecular populations of the two contracted d functions and the ratio of the three in the free atom. The difference of this 'expected' atom-like population from the actually calculated diffused population we have called the 4d* popu-

Table 2 Summary of spin populations given by the reduced chemical model fitting of the experiment (units e) and the results from the *ab-initio* calculations

		Theory			
Atom	Experiment	HF Non-relativistic all-electron	HF Relativistic pseudo-potential	LDF Non-relativistic all-electron	LDF[10] Relativistic pseudo-potential
Tc $4d_{xy}$	0.62(3)	0.88	0.88	0.63	0.64
other 4d	0.13(3)	0.08	0.09	0.28	0.15
5s/p	—	0.01	0.00	0.03	0.03
Cl	0.079(6)	0.018	0.020	0.074	0.072
N	−0.133(17)	−0.051	−0.049	−0.244	−0.124
H	0.005(2)	—	—	—	—

Table 3 Values of the fitted parameters for the reduced chemical model (units e) and the Amsterdam density functional calculation

Atom		Experiment	Theory
Tc	$4d_{xy}$	0.77(2)	0.69
	$4d_{xz+yz}$	0.08(2)	0.10
	$4d_{x^2-y^2}$	0.03(2)	0.04
	$4d_{z^2}$	0.00(2)	0.03
	*r*4d (κ)	1.00(1)	—
	$4d^*_{xy}$	−0.15(2)	−0.06
	$4d^*_{xz+yz}$	0.14(3)	−0.01
	$4d^*_{x^2-y^2}$	−0.18(3)	0.00
	$4d^*_{z^2}$	0.05(3)	0.00
	*r*4d* (κ)	1.30(5)	—
	multipole (10)	−0.13(2)	—
Cl	$3p_x$	−0.008(5)	−0.016
	$3p_y$	0.069(5)	0.080
	$3p_z$	0.018(4)	−0.001
	d	—	−0.004
N	$2p_\sigma$	−0.012(10)	−0.025
	$2p_\pi$	−0.122(16)	−0.100
	d_π	—	0.001

lation. The latter is thus a measure of the change in shape of the molecular 4d spin at diffuse radii from the free-atom spin shape. It is thus comparable, though not identically defined, to the diffuse function in the fitting of the experimental data.

Discussion

Magnetisation distribution

First we discuss the total magnetisation density, which in this case, can be identified as the spin density since we have an isotropic *g* tensor of 2.00. From Fig. 2 the majority of the spin density on the $TcNCl_4$ fragment lies in a $4d_{xy}$-like distribution on the Tc atom, as a simple ionic crystal-field model predicts. However, in addition, there are clear features due to covalence and spin polarisation, an electron-correlation effect. In Fig. 2 there is noticeable spin density delocalised onto the chlorine in-plane 3p orbital. There is little covalence on the chlorine $3p_\sigma$ or out-of-plane $3p_\pi$ orbitals. In addition in Fig. 3 we see very substantial negative spin density on the nitrogen and positive density on the Tc atom in areas not populated by the $4d_{xy}$ density. This is clear evidence of spin polarisation of Tc–N bonding orbitals. Lastly, the maps show a distinctly negative area in the Tc–Cl bond in the overlap region. Thus the qualitative interpretation of the maps already requires both covalence and electron correlation to be highly significant.

For a more quantitative interpretation we turn to the results of the refinement, which in turn implies a partitioning of spin density between atomic centres. The partitioning is not unique, but in this case the low correlation coefficients between differently atom-centred populations resulting from the relatively contracted radial distributions used in the fit make it quite convincing.

The small magnetic exchange present in the crystal is reflected in the negligible spin density delocalised off the $[TcNCl_4]^-$ ion. The spin population on the $TcNCl_4$ fragment is reduced from unity to 0.96(4), with a barely significant 0.04(4) spin in total on the 20 hydrogen sites per Tc.

Within the $TcNCl_4$ fragment the overall atom-centred populations on Tc [0.78(2)], Cl [0.28(2)] and N [−0.14(1)] demonstrate the covalence in the Tc–Cl bond and the spin polarisation in the Tc–N bond. The result for the chlorine population is in reasonable agreement with the 0.2 spin estimated from the ESR results, given the simple model used in deriving that number. We can now see that the 0.45(6) spin on Cl as estimated from a limited PND data set is mainly a result of the substantial Tc–N polarisation. The fraction of the spin not on the superposed Tc plus N atoms is 0.44 = 0.28/(0.78 − 0.14), in good agreement with the previous PND result.[10] The present more extensive data enable us to allow for these extra effects, and to state that 29(2)% of the spin on the $[TcNCl_4]^-$ ion is delocalised onto the chlorines with −15(1)% delocalised onto the nitrogen. Thus neither ESR nor the previous limited PND tells the complete story.

The anisotropy on the atom centres tells us more. On chlorine the π-bonding orbitals together have net positive spin populations, associated with covalent spin delocalisation, resembling the situation we have previously found, for example in the hexacyanochromate(III) ion.[25] However, here we have the added complication of a lower symmetry about the Tc–Cl bond. The in-plane π orbital has a large significant population, while the out-of-plane π population is not significant. This is just what is expected if it is the Tc-centred spin density of the $4d_{xy}$ orbital that is delocalised. On the nitrogen, which interacts with the formally empty $4d_{xz}$, $4d_{yz}$ and $4d_{z^2}$ technetium orbitals, the densities are all negative, due to spin polarisation, with π polarisation dominant. The anisotropy and radial dependence around the Tc atom seems more complex. If we restrict the flexibility of the model (Table 3), the dominant feature is a $4d_{xy}$ positive density of 0.77(2) which is readily understandable as the result of the ligand field. In addition the Tc-centred diffuse d orbitals show significant density, explainable by spin-polarisation effects. The σ- and π-bonding Tc–N orbitals show significant negative density on the nitrogen, and there is positive density mainly in the diffuse Tc-centred $4d_{z^2}$ and $4d_{xz+yz}$ components of these orbitals, 0.05(3) and 0.14(3), with some in the atom-like $4d_{z^2}$ and $4d_{xz+yz}$, 0.00(2) and 0.08(2). Thus, consistent with the nitrogen populations, π interaction dominates. The remaining d-centred orbital, $4d_{x^2-y^2}$ is σ bonding to chlorine, but the diffuse d population of −0.18(3) compared with the atom-like d of 0.03(2) indicates the expected polarisation of the $x^2 - y^2$ density by the nearby *xy* density. The more flexible model subsumes some of these polarisations into 5sp populations, which may not be realistic, and also *via* 4d′ allows core polarisation, making an altogether more complicated result less capable of such simple interpretation. However, the overall improvement in fit when diffuse density is modelled a little less flexibly, while core d populations are more so, indicates that core polarisation of the technetium ion is significant.

Proton-spin polarisation

Our empirical modelling has clearly indicated that there is a proton-spin polarisation which is not significantly different in the two crystal orientations nor over the five independent sites, and which does not change over the 10 d period of the PND experiment. For the magnetic field and temperature of our experiment we predict an equilibrium proton polarisation of 0.31%; 0.28(2)% is observed. This corresponds to a spin temperature of 1.7(1) K, agreeing fairly well with the nominal sample temperature of 1.5 K. This agreement provides confidence in the other results of the refinements. We should also note the sensitivity of PND to proton polarisation in which we obtain an error of only 0.014%.

Theoretical calculation

The unrestricted theoretical calculations, shown in Table 2, all reproduce the qualitative features of the spin density on the $[TcNCl_4]^-$ fragment. That is, the localisation of spin into the technetium $4d_{xy}$ orbital which is covalently bonded to the in-plane chlorine π orbitals and the spin polarisation of the σ and π systems on the N are both reproduced in all calculations. The covalent delocalisation onto the chlorines in the Hartree–Fock calculations is a factor of 2 too small, while the polarisation of the Tc–N bond is too low by an even larger factor. Given that the MIDI-plus-polarisation calculation employs a relatively extensive basis set, it seems unlikely that the discrepancy arises from inadequacy of the basis set (although this basis is not by any means near to the Hartree–Fock limit). It seems more likely that it is the inadequate treatment of electron correlation inherent in the UHF approximation that is a problem. This conclusion is strengthened by the failure to reproduce the sizeable technetium radial polarisations that we see in the experiment. The multiple p and d functions in the valence region of the 15,9,6/6,3,3 MIDI basis are, in principle, capable of duplicating such spin polarisation. Unfortunately, while configuration-interaction calculations are quite feasible on an ion of this size, available packages are unable to extract spin densities from the resulting better correlated wavefunctions.

The simple density functional calculation, by contrast, provides far too much covalence and interatomic spin polarisation. In this calculation the molecular basis is fixed, relatively rigidly, at atom-like functions and the correlation is treated at the lowest density functional approximation. The second density functional calculation is a significant improvement both theoretically and in agreement with experiment. It has both a much more flexible basis, and improved density functional approximations which, among other things, are expected to provide a better treatment of correlation than do the UHF calculations. This improvement seems to provide the key to the better agreement; we need both triple-zeta quality basis sets and a better treatment of electron correlation than the UHF calculation can provide. The use of a relativistic effective core potential may well also be necessary. Even though the interatomic spin polarisations are well described, the intratechnetium polarisation is still not completely correct.

Conclusion

The experimental spin distribution derived by modelling the PND data from this $4d^1$ $[TcNCl_4]^-$ complex clearly quantifies that obtained from previous limited experiment and qualitative theory, *viz.*: (*a*) covalent delocalisation of 29(2)% of the single spin from the technetium $4d_{xy}$ orbital onto the chlorine in-plane $3p_\pi$ orbital region; (*b*) spin polarisation of the Tc–N bond, mainly of π symmetry, resulting in a negative spin population on the nitrogen of −15(1)% of the total; (*c*) more unexpectedly, there is a complex spin polarisation of d electrons on the Tc which results in a shape change of the formally unpaired spin density such that the diffuse fringes of the d density have opposite sign of spin to the majority; in addition the formally spin-paired d-orbital populations are polarised in ways predictable from their bonding or non-bonding nature.

The amount of proton nuclear spin alignment predicted for this high magnetic field and low temperature is also observed in the fit.

Theoretical *ab-initio* calculations must include electron correlation in some way even qualitatively to account for these observations. Our UHF calculations, with reasonable basis sets, reproduce the Tc–Cl covalence and Tc–N spin polarisation qualitatively, but not quantitatively. The spin polarisation on the Tc is not reproduced at all. The inference is that electron correlation must be dealt with better by use of multideterminant wavefunctions and configuration interaction. Simple UHF all-electron or quasi-relativistic effective core potential calculations provide an inadequate description of the bonding in this complex ion.

By contrast, a density functional calculation, which includes a flexible basis set and a relativistic effective core potential, reproduces our results quite well, possibly largely because this method also treats electron correlation more adequately than does the UHF method. The spin densities on the ligand are predicted almost quantitatively, while the complex pattern of spin polarisation on the technetium, which the UHF calculations do not predict at all, are now in semiquantitative agreement with experiment. We are comparing differently defined and obtained populations in the theory and experiment, and the measurements are on a crystal while the calculation is on an isolated ion. It is not clear that better agreement should be expected. A better assessment of theory *versus* experiment would be an Amsterdam density functional band calculation of magnetic structure factors, to compare directly with the experimental values. This is our next task.

Acknowledgements

We thank the Australian Research Council and the Department of Industry, Trade and Tourism for financial support, and the Institut Laue-Langevin for access to the D3 polarised neutron diffractometer.

References

1 B. N. Figgis, J. B. Forsyth, E. S. Kucharski, P. A. Reynolds and F. Tasset, *Proc. R. Soc. London, Ser. A*, 1990, **428**, 113; P. J. Brown, B. N. Figgis and P. A. Reynolds, *J. Phys. Condens. Matter*, 1990, **2**, 5309; C. D. Delfs, B. N. Figgis, J. B. Forsyth, E. S. Kucharski, P. A. Reynolds and M. Vrtis, *Proc. R. Soc. London, Ser. A*, 1992, **436**, 417.
2 P. A. Reynolds, B. Moubaraki, K. S. Murray, J. W. Cable, L. M. Engelhardt, B. N. Figgis and A. N. Sobolev, unpublished work.
3 P. A. Reynolds, B. Moubaraki, K. S. Murray, J. W. Cable, L. M. Engelhardt and B. N. Figgis, *J. Chem. Soc., Dalton Trans.*, 1997, 263.
4 S. P. Best, B. N. Figgis, J. B. Forsyth, P. A. Reynolds and P. L. W. Tregenna-Piggott, *Inorg. Chem.*, 1995, **34**, 4605.
5 J. Baldas, J. F. Boas, J. Bonnyman and G. A. Williams, *J. Chem. Soc., Dalton Trans.*, 1984, 2395.
6 B. N. Figgis, P. A. Reynolds, F. K. Larsen, G. A. Williams and C. D. Delfs, *Aust. J. Chem*, 1996, **49**, 663.
7 J. B. Raynor, T. J. Kemp and A. M. Thyer, *Inorg. Chim. Acta*, 1992, **193**, 191.
8 R. Kirmse, K. Kohler, U. Abram, R. Bottcher, L. Golic and E. de Boer, *Chem. Phys.*, 1990, **143**, 75.
9 K. Kohler, R. Kirmse, R. Bottcher, U. Abram, M. C. M. Gribnau, C. P. Keijzers and E. de Boer, *Chem. Phys.*, 1990, **143**, 83.
10 B. N. Figgis, P. A. Reynolds and J. W. Cable, *J. Chem. Phys.*, 1993, **98**, 7743.
11 H. Glättli and M. Goldman, *Methods Exp. Phys.*, 1987, **23C**, 241.
12 A. Abragam, G. L. Bacchella, C. Long, P. Meriel, J. Peisvaux and M. Pinot, *Phys. Rev. Lett.*, 1972, **28**, 805.
13 M. Leslie, G. T. Jenkin, J. B. Hayter, J. W. White, S. Cox and G. Warner, *Philos. Trans. R. Soc. London, Ser. B*, 1980, **290**, 497 and refs. therein.

14 A. Zheludev, V. Barone, M. Bonnet, B. Delley, A. Grand, E. Ressouche, P. Rey, R. Subra and J. Schweizer, *J. Am. Chem. Soc.*, 1994, **116**, 2019.
15 B. N. Figgis, P. A. Reynolds and G. A. Williams, *J. Chem. Soc., Dalton Trans.*, 1980, 2339.
16 E. Clementi and C. Roetti, *At. Data Nucl. Data Tables*, 1974, **14**, 177.
17 J. M. Stewart, E. R. Davidson and W. T. Simpson, *J. Chem. Phys.*, 1965, **87**, 3175.
18 A. Neuhaus, A. Veldkamp and G. Frenking, *Inorg. Chem.*, 1994, **33**, 5278.
19 P. J. Hay and W. R. Wadt, *J. Chem. Phys.*, 1985, **82**, 299.
20 V. Jonas, G. Frenking and M. T. Reetz, *J. Comput. Chem.*, 1992, **13**, 919.
21 W. J. Hehre, R. Ditchfield and J. A. Pople, *J. Chem. Phys.*, 1972, **56**, 2257.
22 M. W. Schmidt, K. K. Baldridge, J. A. Boatz, S. T. Elbert, M. S. Gordon, J. H. Jensen, S. Kaseki, N. Matsunaga, K. A. Nguyen, S. J. Su, T. L. Windus, M. Dupuis and J. A. Montgomery, *J. Comput. Chem.*, 1993, **14**, 1347.
23 *Gaussian basis sets for molecular calculations*, eds. S. Huzinaga, J. Andzelm, M. Klobukowski, E. Radzio-Andzelm, Y. Sakai and H. Tatewaki, Elsevier, Amsterdam, 1984.
24 C. Fonseca Guerra, in *Methods and Techniques in Computational Chemistry*, eds. E. Clementi and G. Corongiu, STEF, Cagliari, 1995; G. te Velde and E. J. Baerends, *J. Comput. Phys.*, 1992, **99**, 84; E. J. Baerends, D. E. Ellis and P. Ros, *Chem. Phys.*, 1973, **2**, 41.
25 B. N. Figgis, J. B. Forsyth and P. A. Reynolds, *Inorg. Chem.*, 1987, **26**, 101.

Received 11*th November* 1996; *Paper* 6/07650E